HHS Public Access

Author manuscript

Nanotoxicology. Author manuscript; available in PMC 2025 September 19.

Published in final edited form as:

Nanotoxicology. 2024 September ; 18(6): 565–581. doi:10.1080/17435390.2024.2404074.

HMGB1 derived from lung epithelial cells after cobalt nanoparticle exposure promotes the activation of lung fibroblasts

Jiali Yuan[*,1], **Yiqun Mo**[*,1], **Yue Zhang**[2], **Yuanbao Zhang**[1], **Qunwei Zhang**[1]

[1]Department of Epidemiology and Population Health, School of Public Health and Information Sciences, University of Louisville, Louisville, KY, USA.

[2]Indiana University School of Medicine, Indianapolis, IN, USA.

Abstract

We have previously demonstrated that exposure to cobalt nanoparticles (Nano-Co) caused extensive interstitial fibrosis and inflammatory cell infiltration in mouse lungs. However, the underlying mechanisms of Nano-Co-induced pulmonary fibrosis remain unclear. In this study, we investigated the role of high-mobility group box 1 (HMGB1) in the epithelial cell-fibroblast crosstalk in Nano-Co-induced pulmonary fibrosis. Our results showed that Nano-Co exposure caused remarkable production and release of HMGB1, as well as nuclear accumulation of HIF-1α in human bronchial epithelial cells (BEAS-2B) in a dose- and a time-dependent manner. Pretreatment of CAY10585, an inhibitor against HIF-1α, significantly blocked the overexpression of HMGB1 in cell lysate and the release of HMGB1 in the supernatant of BEAS-2B cells induced by Nano-Co exposure, indicating that Nano-Co exposure induces HIF-1α-dependent HMGB1 expression and release. In addition, treatment of lung fibroblasts (MRC-5) with conditioned media from Nano-Co-exposed BEAS-2B cells caused increased RAGE expression, MAPK signaling activation, and enhanced expression of fibrosis-associated proteins, such as fibronectin, collagen 1, and α-SMA. However, conditioned media from Nano-Co-exposed BEAS-2B cells with HMGB1 knockdown had no effects on the activation of MRC-5 fibroblasts. Finally, inhibition of ERK1/2, p38, and JNK all abolished MRC-5 activation induced by conditioned media from Nano-Co-exposed BEAS-2B cells, suggesting that MAPK signaling might be a key downstream signal of HMGB1/RAGE to promote MRC-5 fibroblast activation induced by Nano-Co. These findings have important implications for understanding the pro-fibrotic potential of Nano-Co.

Address correspondence to: Qunwei Zhang, MD, MPH, PhD, Department of Epidemiology and Population Health, School of Public Health and Information Sciences, University of Louisville, 485 E. Gray Street, Louisville, KY 40202, Fax: (502)852-7246, Qunwei.Zhang@louisville.edu.

*Yuan J. and Mo Y. contributed equally to this work.

Authors' contributions

JY, YM, YBZ, and YZ designed and performed the experiments, analyzed the data, and/or interpreted the results of the experiments. QZ conceived and supervised the study. The manuscript was written by JY, YM, and YZ and revised critically by QZ. All authors read and approved the final manuscript.

Disclosure statement

The authors declare that they have no known competing financial interests or personal relationships that could have appeared to influence the work reported in this paper.

Keywords

Metal nanoparticles; High-mobility group box 1 (HMGB1); Hypoxia inducible factor-1α (HIF-1α); Receptor for advanced glycation end-products (RAGE); Mitogen-activated protein kinases (MAPKs)

Introduction

Cobalt nanoparticles (Nano-Co) have a wide range of industrial applications, such as metal ceramics, diamond tools, hominess alloy, ferrofluids, and so on (Dutz et al. 2020; Milikić et al. 2022; Simm et al. 2006; Younus et al. 2019). In the field of biomedicine, magnetic nanoparticles, including Nano-Co, have also been used as effective contrast agents for magnetic resonance imaging (MRI) and for the ablation of tumors through magnetic thermotherapy (Perez et al. 2020). Cobalt is a relatively rare magnetic element with non-negligible health hazards of carcinogenicity, sensitization, and pro-fibrogenesis (Lison et al. 2001; Nemery 1990; Thyssen 2012). Cobalt metal and soluble cobalt(II) salts were classified as "probably carcinogenic to humans" (Group 2A) by the International Agency for Research on Cancer (IARC) (IARC. 2023; Middleton et al. 2024). Individuals are at risk for multiple routes of cobalt exposure, including inhalation, ingestion, skin, and/or eye contact. According to the Pocket Guide to Chemical Hazards released by the National Institute for Occupational Safety and Health (NIOSH), the recommended exposure limit (REL) for cobalt metal dust and fume is 0.05 mg/m^3 (TWA) (https://www.cdc.gov/niosh/npg/npgd0146.html). However, the occupational exposure limits for Nano-Co are not yet clearly defined. Thus, more evidence from epidemiological and toxicological investigations is urgently required for the risk assessment and exposure control of Nano-Co.

Cobalt or its compounds have shown acute toxicity both *in vitro* and *in vivo* (Simonsen et al. 2012). The release of high concentrations of cobalt ions (Co^{2+}) from cobalt-chromium (Co-Cr) alloys induced apoptosis, necrosis, and inflammatory responses in lymphocytes and macrophages (Akbar et al. 2011; Kwon et al. 2009). Yet nano-scaled metal particles usually exhibited different or even stronger toxic effects than their micro- or bulk-sized particles (Brown et al. 2013; Zhang et al. 2000). Current toxicological evidence has revealed the neurotoxic, genotoxic, and carcinogenic potential of cobalt-based nanoparticles and partially elucidated the underlying mechanisms, including enhanced oxidative stress, inflammasome activation, and genomic DNA damage (Feng et al. 2020; Lin et al. 2024). Lin et al. recently documented the neurotoxicity of Nano-Co by stimulating the excessive production of mitochondrial ROS and the activation of PI3K/AKT/mTOR signaling in glioma cells (Lin et al. 2024). Our previous investigation revealed that exposure to Nano-Co upregulated levels of DNA damage markers, including γ-H2AX, 8-OHdG, and ATM, both in mouse lung tissues and human lung epithelial cells (Wan et al. 2012; Wan et al. 2017). Notably, intratracheal instillation of Nano-Co caused massive inflammatory cell infiltration, focal proliferation of alveolar epithelial cells, alveolar septal thickening, and finally fibrosis in mouse lung tissues (Wan et al. 2017). However, the underlying mechanisms of Nano-Co-induced pulmonary fibrosis are still unknown and need further exploration.

The aberrant interaction between lung epithelial cells and lung fibroblasts was considered crucial to tissue homeostasis and the development of pulmonary fibrosis (Xu et al. 2018; Zhang et al. 2023). Sustained and repeated injury drives epithelial cells to release damage-associated molecular patterns (DAMPs), including high mobility group box-1 (HMGB1), which could, in turn, trigger fibroblast activation and extracellular matrix (ECM) deposition, a key initiating event in lung fibrosis (Isshiki et al. 2024). In this study, we focused on the role of HMGB1 in epithelial cell-fibroblast interactions in the development of Nano-Co-induced pulmonary fibrosis. HMGB1 belongs to the high-mobility group box protein family, which is the first described DAMP (Rarick et al. 2024). HMGB1 could sense and coordinate the cellular stress responses, thus playing a protective role in chromatin stabilization, autophagy maintenance, and anti-cell death inside the cells, and acting as a pro-inflammatory and pro-fibrosis stimulus outside (Kang et al. 2014). Significantly higher levels of HMGB1 in the alveolar lavage fluid of patients with pulmonary fibrosis have been observed as compared to the controls (Hamada et al. 2008). *In vivo* studies also indicated that bleomycin administration induced a remarkable increase in HMGB1 production in the mouse lungs (He et al. 2007; Kida et al. 2018). In addition, the treatment of recombinant HMGB1 protein (250 and 1000 ng/mL) significantly promoted the fibrotic transformation of human fetal lung fibroblasts (MRC-5) (Hou et al. 2015). However, whether Nano-Co exposure could elevate the expression and release of HMGB1 in human bronchial epithelial cells, thus leading to pulmonary fibroblast activation is still unclear.

In the present study, we investigated the potential mechanisms underlying Nano-Co-induced lung fibroblast activation and pulmonary fibrosis. First, we focused on the production and secretion of HMGB1 in BEAS-2B cells exposed to Nano-Co and the potential mechanisms. Subsequently, conditioned media from Nano-Co-exposed BEAS-2B cells with or without HMGB1 knockdown was applied to culture MRC-5 fibroblasts, and the expressions of fibrosis-associated proteins in MRC-5 cells were determined to explore whether BEAS-2B-derived secretory HMGB1 could activate MRC-5 fibroblasts. We also examined the expression of RAGE, an HMGB1 receptor, and phosphorylation levels of MAPK signaling proteins in MRC-5 fibroblasts cultured in conditioned media. Titanium dioxide nanoparticles (Nano-TiO_2) were used as a nanoparticle control, as our previous studies showed that Nano-TiO_2 exposure elicited only a minor and negligible HIF-1α nuclear accumulation and fibrotic response (Wan et al. 2017; Yuan et al. 2022).

Materials and methods

Chemicals and reagents

HMGB1 (D3E5) Rabbit mAb #6893 (1:1000), β-Actin (E4D9Z) Mouse mAb #58169 (1:1000), RAGE (E7I6S) Rabbit mAb #55222 (1:1000), p44/42 MAPK (Erk1/2) (3A7) Mouse mAb #9107 (1:1000), Phospho-p44/42 MAPK (Erk1/2) (Thr202/Tyr204) Antibody #9101 (1:1000), p38 MAPK Antibody #9212 (1:1000), Phospho-p38 MAPK (Thr180/Tyr182) (3D7) Rabbit mAb #9215 (1:1000), JNK2 (56G8) Rabbit mAb #9258 (1:1000), Phospho-SAPK/JNK (Thr183/Tyr185) (81E11) Rabbit mAb #4668 (1:1000), COL1A1 (E8F4L) Rabbit mAb #72026 (1:1000), Fibronectin/FN1 (E5H6X) Rabbit mAb #26836 (1:1000), anti-mouse IgG, HRP-linked antibody #7076 (1:1000), and anti-rabbit IgG, HRP-

linked antibody #7074 (1:1000) were obtained from Cell Signaling Technology (Beverly, MA, USA). Mouse anti-human HIF-1α #610958 (1:1000) was obtained from BD (San Jose, CA, USA). α-SMA Mouse mAb #A5228 (1:4000) was from SIGMA (Saint Louis, MO, USA). The above dilution ratios for the antibodies were for Western blot. Alexa Fluor 488-conjugated goat anti-mouse IgG (#A1101, 1:500) was purchased from Invitrogen (Carlsbad, CA, USA) and Alexa Fluor 594-conjugated donkey anti-rabbit IgG (#ab150076, 1:500) was from Abcam (Cambridge, MA, USA).

CAY10585 was obtained from BioVision (Milpitas, CA, USA). HMGB1 siRNA (sc-37982) and control siRNA (sc-37007) were purchased from Santa Cruz (CA, USA). PD98059 and SB203580 were obtained from TOCRIS (Ellisville, MO, USA), and SP600125 from Fisher Scientific (Fair Lawn, NJ, USA). All other chemicals were purchased from Fisher (Pittsburgh, PA, USA) unless otherwise indicated.

Metal nanoparticle characteristics

Nano-Co and Nano-TiO_2 used in this study were obtained from INABTA and Co., Ltd., Vacuum Metallurgical Co., Ltd., Japan. The detailed characterization of both kinds of metal nanoparticles has been described in our previous publications (Feng et al. 2015; Wan et al. 2012). Briefly, the mean diameter of Nano-Co is 20 nm, and Nano-TiO_2 is 28 nm. The specific surface area of Nano-Co or Nano-TiO_2 is 47.9 m^2/g or 45.0 m^2/g, respectively. Nano-Co is composed of 85-90% of metal Co and 10-15% of Co_3O_4. Nano-TiO_2 is composed of 90% of anatase and 10% of rutile. The mean size of particles and agglomerates in cell culture medium is 260 nm for Nano-Co and 280 nm for Nano-TiO_2, measured by dynamic light scattering (DLS). After 1 mg/mL of Nano-Co or Nano-TiO_2 was shaken for 48 h in a 37°C water bath, the supernatant was collected to determine the concentration of cobalt or titanium ion by inductively coupled plasma−atomic emission spectrometry (ICP-AES). The solubility of Nano-Co is 10.81 ± 0.62 ppm in PBS and 45.35 ± 1.68 ppm in cell culture medium, while the solubility of Nano-TiO_2 is <1.00 ppm in both PBS and cell culture medium (Wan et al. 2012). Nano-Co and Nano-TiO_2 were dispersed in physiological saline and were ultrasonicated for at least 10 min before being added to the cells.

Cytotoxicity assays

The cytotoxicity of Nano-Co and Nano-TiO_2 on BEAS-2B cells was measured by an *In Vitro* cytotoxicity assay kit (Sulforhodamine B Based, Sigma-Aldrich, St Louis, MO) (SRB assay) and the alamarBlue™ assay (Invitrogen, Eugene, OR) according to the manufacturer's instructions. Briefly, 100 μL of cell suspension was added into each well of a 96-well plate (5×10^3 cells/per well) and cultured overnight for cell attachment to the growth surface. The cells were then treated with 0, 1.25, 2.5, 5.0, 7.5, and 10 μg/mL of Nano-Co or Nano-TiO_2 in a total volume of 200 μL per well for another 24 h. The cell images were captured under a microscope (Olympus, model IX51). For SRB assay, the cells were fixed with 50 μL pre-cooled 50% trichloroacetic acid (TCA) for 1 h at 4°C. After being rinsed 5 times with ddH_2O and dried at room temperature (RT), the cells were dyed with 50 μL of 0.4% SRB (Sulforhodamine B Solution) for 30 min. The free SRB dye was washed away with 1% acetic acid for 5 times, and the plate was dried at RT. Bound SRB was dissolved in 150 μL of 10 mM Tris-Base solution (pH 7.4), and the plate was shaken for 5 min at dark. The

absorbance was measured by Synergy HT microplate reader (BioTek, Winooski, VT, USA). The absorbance of each sample was calculated as the absorbance measured at a wavelength of 565 nm minus the background absorbance measured at a wavelength of 690 nm. For the alamarBlue assay, the cells were stained with alamarBlue dye for 2 hours and then subjected to the measurement of the fluorescence absorbance (λex530 nm/λem590 nm) by Synergy HT microplate reader.

The viability of MRC-5 cells was determined by CellTiter 96 AQueous Non-Radioactive Cell Proliferation Assay (MTS assay, Promega, Madison, WI, USA). Briefly, a total volume of 100 μL cell suspension containing 2×10^3 cells was added into each well of a 96-well plate. After cell attachment to the growth surface, the cells were continuously incubated with a conditioned medium for 24, 48, and 72 h. Then, 20 μL MTS working solution was added to each well and the cells were incubated for another 2 hours at 37°C before absorbance measurement at 490 nm by Synergy HT microplate reader.

Cell culture and transfection

Normal human bronchial epithelial cells BEAS-2B (#CRL-9609) and lung fibroblasts MRC-5 (#CCL-171) were purchased from American Type Culture Collection (ATCC, Manassas, VA, USA) and cultured in RPMI 1640 medium and Eagle's Minimum Essential medium (EMEM) supplemented with 10 % fetal bovine serum (FBS), 100 U/mL of penicillin, and 100 μg/mL of streptomycin. Cells were maintained in an incubator with a humidified atmosphere of 5% CO_2 at 37 °C.

To collect conditioned media for MRC-5 fibroblast culture, BEAS-2B cells were pre-cultured in an FBS-free medium for 24 h. After being treated with metal nanoparticles, the FBS-free conditioned media were collected and centrifuged at 1,000 *g* for 10 min. Then the conditioned media were added to complete EMEM in a 1:1 ratio to culture MRC-5 fibroblasts for 24, 48, or 72 h. For transfection, the BEAS-2B cells were seeded into 6-well plates (Corning, Manassas, VA, USA) at a density of 2×10^5 cells per well and cultured overnight for cell adherence. 5 μL of HMGB1 or Control siRNA (20 μM) was mixed with 10 μL of Lipofectamine™ 2000, and the mixture was incubated for 15 min at room temperature. The cells were then cultured with 2 mL serum-free medium containing the above mixture for 24 h. Subsequently, the culture medium was refreshed with or without 5 μg/mL of Nano-Co, and the cells were maintained culturing for 24 h before the cells and the culture media were collected for further analysis.

Protein extraction and Western blot

Proteins of cells were extracted by RIPA buffer (Santa Cruz, CA, USA) for the determination of intracellular HMGB1, RAGE, fibrosis-associated proteins, and MAPKs. Conditioned medium was collected and concentrated by Amicon® Ultra Centrifugal Filters (Millipore, Burlington, MA, USA) for the determination of the secreted HMGB1 level. Nuclear protein was extracted from the cells using NE-PER® Nuclear and Cytoplasmic Extraction Reagent (Thermo Scientific, Rockford, IL, USA) to detect the expression of HIF-1α. Western blot was performed as described in our previous study (Yuan et al. 2021). Immunoreactive bands were detected using SuperSignal™ West Pico PLUS

Chemiluminescent Substrate (Thermo Scientific, Rockford, IL, USA) followed by exposure to CL-XPosure™ film (Thermo Scientific). Equal nuclear protein and supernatant protein loading were verified by Coomassie Brilliant Blue staining. β-actin was used as an internal reference for protein expression in the cells. Immunoreactive bands were quantified using NIH ImageJ software (http://imagej.nih.gov/ij/).

RNA extraction and quantitative real-time PCR

Total RNA was extracted from BEAS-2B cells using Trizol reagent (Sigma-Aldrich, St Louis, MO, USA) according to the manufacturer's instructions. The concentration and quality of the RNA were determined using a spectrophotometer (Beckman Coulter, Fullerton, CA, USA). Complementary DNA (cDNA) of genes were generated by reverse-transcription from total RNA using M-MLV reverse transcriptase (Promega, Madison, WI, USA) and oligo (dT)18 (Sigma), and the iTaq™ Universal SYBR® Green Supermix (Bio-Rad, Hercules, CA, USA) was used for amplification. PCR analysis was performed by the Bio-Rad iQ5 Multicolor Real-Time PCR Detection System (Bio-Rad). Data were quantified by the $2^{-\Delta\Delta Ct}$ (Livak) method (Schmittgen and Livak 2008). The PCR reaction was performed as follows: 35 cycles at 94 °C for 45 s, at 58 °C for 45 s, and at 72 °C for 45 s. The primers for human HMGB1 were forward 5'-TAT GGC AAA AGC GGA CAA GG-3' and reverse 5'-CTT CGC AAC ATC ACC AAT GGA-3', and for human β-actin were forward 5'-CAT CGA GCA CGG CAT CGT CA-3' and reverse 5'-TAG CAC AGC CTG GAT AGC AAC-3'.

Dual immunofluorescent staining

MRC-5 cells were seeded in 2-well LAB-TEK® chamber slides (Nalge Nunc International, Rochester, NY), and BEAS-2B cells were seeded in 6-well plates. After overnight culture for cell attachment, the BEAS-2B cells were treated with 5 μg/mL of Nano-Co or TiO_2 for 24 h in a FBS-free medium. Then the conditioned media were collected, centrifuged, and 1:1 mixed with complete EMEM to culture MRC-5 cells for 48 h. At the end of the experiment, MRC-5 cells were fixed in 10% neutral buffered formalin for 20 min at room temperature and washed with 1x PBS for three times with 5 min for each time. The cells were incubated with a blocking solution containing 3% BSA, 5% normal donkey serum, and 0.3% Triton X-100 for 1 h at room temperature. Then the cells were incubated with primary antibodies α-SMA (1:400) and COL1A1 (1:200) for 3 h at room temperature. After washing with 1x PBS three times, the cells were incubated with Alexa Fluor 488-conjugated goat anti-mouse IgG (1:500) and Alexa Fluor 594-conjugated donkey anti-rabbit IgG (1:500) at room temperature for 1 h. After washing, the slides were mounted with Prolong Gold Antifade Reagent with DAPI (Invitrogen, Carlsbad, CA, USA) and images were captured under fluorescence microscopy (Nikon, Japan).

Statistical analysis

SigmaPlot 13.0 (Systat Software, San Jose, CA) was used for data management and statistical analysis in this study. All the data were presented as the mean ± SE. The differences among groups were calculated by one-way ANOVA followed by Dunnett's Test. $P < 0.05$ was considered statistically significant.

Results

Cytotoxic effects of Nano-Co and Nano-TiO_2 on BEAS-2B cells

BEAS-2B cells were exposed to 1.25, 2.5, 5.0, 7.5, and 10 μg/mL of Nano-Co or Nano-TiO_2 for 24 h, and the cell viability was determined by both SRB assay and alamarBlue assay. Exposure of BEAS-2B cells to Nano-Co at 7.5 μg/mL and beyond caused significant cell death by SRB assay, while exposure to 5 μg/mL or less of Nano-Co did not cause significant cell death (Figure 1(A)). However, exposure of BEAS-2B cells to doses from 0 to 10 μg/mL of Nano-TiO_2 did not cause significant cytotoxic effects (Figure 1(A)). The results were further confirmed by alamarBlue assay (Figure 1(B)). The cell images were shown in Figure 1(C). In the following experiments, the non-cytotoxic doses (≤ 5 μg/mL) were selected to explore the effects of Nano-Co on BEAS-2B cells.

Exposure of BEAS-2B cells to Nano-Co caused increased expression and release of HMGB1

The mRNA expression of HMGB1 in BEAS-2B cells exposed to Nano-Co or Nano-TiO_2 was determined by real-time PCR. The results showed that HMGB1 mRNA levels in BEAS-2B cells were considerably enhanced by 2.5 and 5 μg/mL of Nano-Co exposure for 24 h or by 5 μg/mL of Nano-Co exposure for 12, 24, and 48 h, whereas Nano-TiO_2 exposure had no effects on HMGB1 mRNA levels (Figure 2(A,B)). In line with the changes in HMGB1 mRNA, BEAS-2B cells treated with 2.5 and 5 μg/mL of Nano-Co for 24 h or with 5 μg/mL of Nano-Co for 12, 24, or 48 h showed a substantial increase in HMGB1 protein levels in both the lysate and cell culture supernatant (Figure 2(C-F)). Additionally, there were no discernible changes in the expression of HMGB1 protein after Nano-TiO_2 exposure (Figure 2(C,D)).

Nano-Co exposure caused HIF-1α nuclear accumulation in BEAS-2B cells, and HIF-1α inhibition abolished Nano-Co-induced upregulation and release of HMGB1

We examined the nuclear accumulation of HIF-1α in BEAS-2B cells after Nano-Co exposure. Western blot results showed that 2.5 and 5 μg/mL of Nano-Co treatment for 24 h or 5 μg/mL of Nano-Co treatment for 6, 12, 24, and 48 h induced a dose- and a time-dependent HIF-1α nucleus accumulation (Figure 3(A-D)). However, exposure of BEAS-2B cells to Nano-TiO_2 did not cause HIF-1α nuclear accumulation (Figure 3(A,B)).

The hypoxic environment was considered to favor HMGB1 expression and release (Peng et al. 2021; Tohme et al. 2017). Our previous studies revealed that Nano-Co exposure significantly induced the nuclear accumulation of HIF-1α in mouse embryo fibroblasts (Feng et al. 2015), and here we showed that Nano-Co exposure caused HIF-1α nuclear accumulation in human lung epithelial cells BEAS-2B. Thus, we hypothesized that the nuclear accumulation of HIF-1α might have a crucial role in the production and release of HMGB1 from Nano-Co-exposed BEAS-2B cells. To address that, CAY10585, a novel HIF-1α inhibitor, was applied to suppress the HIF-1α nuclear accumulation. CAY10585 has been proven to promote proteasomal degradation of HIF-1α by upregulating von Hippel-Lindau (VHL) without affecting HIF-1β expression (Lee et al. 2010; Lee et al. 2007). BEAS-2B cells were pretreated with 30 μM of CAY10585 for 2 h before being exposed

to 5 μg/mL Nano-Co for 24 h. As expected, pretreatment with CAY10585 significantly reduced the nuclear accumulation of HIF-1α (Figure 4(A,B)). Furthermore, CAY10585 administration markedly restrained HMGB1 mRNA level (Figure 4(C)) and the production and release of HMGB1 protein (Figure 4(D,E)) in BEAS-2B cells exposed to Nano-Co.

Conditioned medium from Nano-Co-exposed BEAS-2B cells elevated the viability of MRC-5 fibroblasts and promoted the expression of fibrosis-associated proteins

Next, we investigated the effects of the conditioned media from BEAS-2B cells exposed to Nano-Co or Nano-TiO_2 on the activation of MRC-5 fibroblasts. The serum-free RPMI 1640 medium for culturing BEAS-2B cells was collected and centrifugated, and the supernatant was then mixed with EMEM medium in a 1:1 ratio to culture MRC-5 fibroblasts (Figure 5(A)). We first measured the cell viability of MRC-5 fibroblasts after conditioned medium culture by MTS assay. The results showed that culture of MRC-5 cells with conditioned media from Nano-Co-exposed BEAS-2B cells remarkably enhanced cell viability, indicating the activation of MRC-5 cells (Figure 5(B)). Wherevers, cells cultured with conditioned media from BEAS-2B cells exposed to Nano-TiO_2 showed no changes in the cell viability of MRC-5 cells compared to the control group (Figure 5(B)). Furthermore, the expressions of fibrosis-associated proteins, such as fibronectin, collagen 1, and α-SMA, were also examined. The results of Western blot demonstrated that fibronectin, collagen 1, and α-SMA all exhibited marked increases in MRC-5 cells after the cells were cultured with conditioned media from Nano-Co-exposed BEAS-2B cells (Figure 5(C-F)). The enhanced expressions of α-SMA and collagen 1 in MRC-5 cells cultured in conditioned media from Nano-Co-exposed, but not Nano-TiO_2-exposed BEAS-2B cells were further confirmed by immunofluorescence staining (Figure 5(G)).

Knocking down HMGB1 attenuated MRC-5 fibroblast activation caused by culturing with conditioned medium from Nano-Co-exposed BEAS-2B cells

We have revealed that exposure to Nano-Co promoted HMGB1 release from BEAS-2B cells and the conditioned medium from Nano-Co-exposed BEAS-2B cells significantly activated MRC-5 fibroblasts. To investigate the potential role of HMGB1 in the activation of MRC-5, HMGB1 was knocked down in BEAS-2B cells by transfection with siRNA targeting HMGB1. After transfection with HMGB1 siRNA, the intracellular level of HMGB1 protein was significantly suppressed, and the secreted HMGB1 protein in the culture medium became almost unprobeable (Figure 6(A,B)). MRC-5 cells were cultured in conditioned media from BEAS-2B cells with or without HMGB1 knockdown. The proliferation of MRC-5 cells cultured in the conditioned medium from HMGB1-suppressed BEAS-2B cells was significantly attenuated compared to cells culturing in the conditioned medium from control siRNA-transfected BEAS-2B cells (Figure 6(C)). The expression of fibrosis-associated proteins also showed a similar trend, that is, the protein levels of fibronectin, collagen 1, and α-SMA in MRC-5 cells treated with conditioned media from Nano-Co-exposed BEAS-2B cells with HMGB1 siRNA transfection were significantly lower than that of control siRNA and Nano-Co-exposed BEAS-2B cells (Figure 6(D,E)). These results suggest that HMGB1 secreted from Nano-Co-exposed BEAS-2B cells may play a key role in the activation of lung fibroblasts.

HMGB1 released from Nano-Co-exposed BEAS-2B cells activated MRC-5 cells via RAGE/MAPKs pathway

The receptor for advanced glycation end-products (RAGE) is an important signaling receptor highly expressed in lung tissues and closely associated with persistent damage to lung parenchyma and fibrosis (Perkins and Oury 2021). To examine whether RAGE was involved in the Nano-Co-induced HMGB1 production in the epithelial cells and its role in the MRC-5 activation, we subsequently examined the protein level of RAGE, a receptor for HMGB1, and the activation of downstream MAPK signaling in MRC-5 cells cultured with the conditioned media. Our results showed that the conditioned media from Nano-Co-exposed BEAS-2B cells effectively upregulated the protein level of RAGE and the phosphorylated ERK, p38, and JNK in MRC-5 cells (Figure 7(A,B)). In contrast, the protein level of RAGE and phosphorylation levels of ERK, p38, and JNK were significantly inhibited in MRC-5 cells cultured with the conditioned media from HMGB1-suppressed BEAS-2B cells with Nano-Co exposure (Figure 7(A,B)). To further clarify the roles of MAPK signaling pathway in MRC-5 cell activation after HMGB1/RAGE binding, three inhibitors that specifically inhibit ERK, p38, and JNK phosphorylation (PD98059, SB203580, and SP600125) were used to pretreat MRC-5 cells prior to culture with conditioned media. Notably, pretreatment of all three inhibitors showed resistance in MRC-5 cells to the activation induced by conditioned media from Nano-Co-exposed BEAS-2B cells (Figure 7(C,D)), suggesting that MAPK pathway activated by HMGB1 upon binding to RAGE is essential for the MRC-5 fibroblast activation.

Discussion

Occupational exposure to cobalt, usually in combination with other materials, can cause asthma, interstitial pneumonitis, and even pulmonary fibrosis (Adams et al. 2017). Our and other's previous studies also showed that exposure to Nano-Co caused pulmonary inflammation, injury, DNA damage and mutation, cell proliferation, and pulmonary fibrosis (Sisler et al. 2016; Wan et al. 2017; Zhang et al. 2000). Exposure to Nano-CO caused pathological alterations associated with pulmonary fibrosis, including elevated infiltration of inflammatory cells, proliferation of alveolar epithelial cells, interstitial thickening, and collagen deposition (Wan et al. 2017). However, the mechanisms underlying Nano-Co-induced fibrogenic effects are still unclear. In the current study, we first examined the expression of the DAMP molecule, HMGB1, in Nano-Co-exposed BEAS-2B cells and then investigated the role of HMGB1 in MRC-5 fibroblast activation and the underlying potential mechanisms.

Our cytotoxicity study showed that exposure of BEAS-2B cells to 7.5 μg/mL or more of Nano-Co for 24 h caused a significant cytotoxicity. However, exposure to Nano-TiO_2 did not cause any cytotoxic effects at all experiment doses. Although it is not easy to estimate the degree of human health effects at such concentrations or quantities of Nano-Co that might be exposed from dose-response studies, Nano-Co may accumulate in the body. In addition, the results from dose-response studies can help us to choose non-cytotoxic doses to identify the potential biological effects of Nano-Co other than those due to cytotoxicity itself.

The release of various cytokines or exosomes by stressed lung epithelial cells has been shown to cause fibroblasts to display the myofibroblast phenotype or an inflammatory response (Kadota et al. 2022; Sakai and Tager 2013; Yang et al. 2024). For example, in response to cigarette smoke extract (CSE) exposure, airway epithelial cells from COPD patients strongly secreted interleukin 1, which is directly linked to an inflammatory phenotype in fibroblasts (Osei et al. 2016). Human rhinovirus (HRV)-infected airway epithelial cells can secrete interleukin 1α through the secretion of fibroblast-chemotactic CXCL10 and CXCL8, which then leads to the thickening of the lamina reticularis by recruiting fibroblasts (Shelfoon et al. 2016). These results not only showed the crucial roles of epithelial cell-fibroblast crosstalk in the process of lung inflammation and fibrosis but also suggested that there might be significant differences in the production of fibroblast-responsive substances derived from epithelial cells exposed to different stimuli. Since the nucleoplasmic translocation and the release of HMGB1 were closely related to oxidative stress and hypoxia, both of which are involved in Nano-Co-induced various toxic effects (Cheng et al. 2017; Kawamura et al. 2023; Kim et al. 2017), therefore, we first examined the expression and release of HMGB1 in Nano-Co-exposed BEAS-2B cells. Our results indicated that Nano-Co exposure not only induced upregulation of intracellular HMGB1 transcription and translation but also promoted HMGB1 release.

Cobalt exposure leads to substantial HIF-1α-dependent dysregulation of gene expression (Befani et al. 2013). Cobalt chloride has been widely used as an inducer of chemical hypoxia and HIF-1α accumulation (Zhang et al. 2024). Our previous study showed that Nano-Co exposure induced a dose- and a time-dependent nuclear accumulation of HIF-1α in mouse embryo fibroblasts (PW cells) (Feng et al. 2015). This study showed that there was a significant increase in HIF-1α nuclear accumulation in BEAS-2B cells exposed to 2.5 and 5 μg/mL of Nano-Co for 24 h or exposed to 5 μg/mL of Nano-Co for 6, 12, 24, and 48 h. Hypoxic conditions can cause an increase in HIF-1α-dependent HMGB1 expression and secretion in human and mouse hepatocellular carcinoma cells, thereby promoting macrophage infiltration and tumor metastasis (Jiang et al. 2018). In addition, hypoxia is a stressor that induces HMGB1 secretion from epithelial cells (Gao et al. 2021; Peng et al. 2021). This raises the intriguing possibility that HIF-1α may be involved in Nano-Co-induced HMGB1 upregulation. In fact, our results showed that the small molecule CAY10585, a HIF-1α inhibitor, effectively reduced HIF-1α accumulation in BEAS-2B cells exposed to Nano-Co. Furthermore, HMGB1 expression and release from BEAS-2B cells after Nano-Co exposure were also decreased once the accumulation of HIF-1α was inhibited by CAY10585.

The lung is a multicellular organ consisting of different kinds of cells. Lung epithelial cells are located at the interface between the environment and the organism and serve many important functions, including barrier protection, fluid balance, clearance of particulate, initiation of immune responses, mucus and surfactant production, and repair following injury (Burgoyne et al. 2021). Therefore, lung epithelial cells constitute the first defense line to protect lung tissues against various stimuli, such as environmental pollution, particles, and microbes. The lung toxic effects caused by particles were shown not only dependent on the exposure but also on the interaction between different cell types, such as macrophages, epithelial cells, and interstitial cells (Sohaebuddin et al. 2010). Recreating the interaction

of epithelial cells with fibroblasts *in vitro* might, therefore, provide a more accurate model of the *in situ* milieu than studying each cell type in isolation. To study whether exposure to Nano-Co could cause fibroblast activation, an indirect co-culture method was adopted to explore the role of Nano-Co-exposed epithelial cells in fibroblast activation. Briefly, the collected conditioned medium from epithelial cells was used to treat fibroblasts. We found that conditioned media from epithelial cells exposed to Nano-Co caused the proliferation of MRC-5 fibroblasts and increased the expression of fibrosis-associated proteins in MRC-5 cells, such as fibronectin, collagen 1, and α-SMA. Although our results showed that exposure to Nano-Co elevated the release of HMGB1 from epithelial cells into the extracellular compartment, whether these epithelial-derived HMGB1 play a role in conditioned medium-induced fibroblast activation needs to be investigated. Therefore, the siRNA targeting HMGB1 was then transfected into BEAS-2B cells. Inhibition of HMGB1 not only effectively reduced or even almost removed the secreted HMGB1 protein from the conditioned medium, but also significantly attenuated the activation of MRC-5 fibroblasts by the conditioned media from Nano-Co-exposed BEAS-2B cells. Although very complex epithelial cell-derived pro-fibrotic mediators have been identified so far, such as interleukin family members, transforming growth factor-β family members, growth and differentiation factor 15 (Gdf15), and others (Peeters et al. 2013; Saint-Criq et al. 2018; Thompson et al. 2006; Wallace and Howie 1999; Zhang et al. 2019), our results suggested that epithelial cell-derived HMGB1 mediated or at least partially mediated the activation of MRC-5 fibroblasts.

HMGB1 treatment had a significant activating effect on fibroblasts originating from multiple organs (Polanská et al. 2012; Su et al. 2014; Zhao et al. 2018). HMGB1 secreted by keratinocytes could promote the expression of nuclear import of MRTF-A, increase the nuclear accumulation of MRTF-A/SRF complexes, and then enhance the activation of α-smooth muscle actin promoter in dermal fibroblasts, leading to hypertrophic scar formation (Zhao et al. 2018). Cardiac fibroblasts/myofibroblasts can also promote collagen overproduction and deposition by activating PKCβ/Erk1/2 through autocrine HMGB1 (Su et al. 2014). HMGB1-deficient vanishing embryonic fibroblasts also exhibit telomere dysfunction, suggesting a crucial role for HMGB1 in maintaining cellular activity (Polanská et al. 2012). Upregulation of the HMGB1/RAGE pathway has been reported in idiopathic pulmonary fibrosis (IPF) or experimental pulmonary fibrosis induced by bleomycin, LPS, arsenic, asbestos, etc., respectively (Li et al. 2015; Wang et al. 2021; Xue et al. 2020; Zhang et al. 2015). Previous *in vitro* studies also showed that exogenous HMGB1 exhibits activating effects on lung fibroblasts, thereby inducing the secretion and accumulation of extracellular matrix (Hou et al. 2015; Zou et al. 2018). RAGE is one of the well-known receptors for HMGB1 (Sims et al. 2010). Although the overall expression of RAGE in IPF and experimental pulmonary fibrosis showed a decreasing trend, enhanced expression of RAGE was demonstrated both in fibroblasts after *in vitro* stimulation of RAGE ligands and fibroblastic lesions of pulmonary fibrosis (Perkins and Oury 2021). Our results showed that an upregulation of RAGE protein in MRC-5 fibroblasts treated with the conditioned medium from Nano-Co-exposed BEAS-2B cells, whereas RAGE expression level in the conditioned medium lacking HMGB1 was not statistically different compared with those from controls.

It has been reported that extracellular HMGB1 triggers intracellular ROS-dependent MAPK pathway after activation of cell membrane RAGE (Al-Kuraishy et al. 2022; Wu et al.

2021). Activation of the MAPK pathway has been shown to be an effective condition for lung fibroblast-myofibroblast transformation (Ahmedat et al. 2013; Gajjala et al. 2021; Yap et al. 2021). Therefore, in this study, we also examined the roles of MAPK pathway in the activation of MRC-5 cells. Our results showed that conditioned media from Nano-Co-exposed BEAS-2B cells promoted the phosphorylation levels of ERK, P38, and JNK in MRC-5 cells, while HMGB1-inhibited conditioned media had no effects on the phosphorylation levels of MAPKs in MRC-5 cells. ERK, p38, and JNK inhibitors all effectively inhibited the activation of MRC-5 cells induced by Nano-Co-exposed BEAS-2B-derived conditioned media.

Conclusions

In summary, our results demonstrated that exposure of BEAS-2B cells to Nano-Co, rather than Nano-TiO_2, caused a remarkable increase in the transcription, translation, and secretion of HMGB1, as well as nuclear accumulation of HIF-1α. Conditioned media collected from Nano-Co-exposed BEAS-2B cells led to fibroblast activation, enhanced RAGE level, and increased phosphorylated MAPKs in MRC-5 fibroblasts. Mechanistically, Nano-Co exposure elevated the production and secretion of HMGB1 in BEAS-2B cells in a HIF-1α dependent manner. The secretory HMGB1 protein mediated or partially mediated the activation of MRC-5 cells through RAGE/MAPKs signaling pathway (Figure 8). These findings suggest a crucial role of HMGB1 in epithelial cell-fibroblast crosstalk in Nano-Co-induced pulmonary fibrosis, which may have important implications for understanding the potential pulmonary toxicity of Nano-Co.

Funding

This work was partly supported by NIH (ES023693, ES028911, and HL147856), KSEF-148-RED-502-16-381, and the Kentucky Lung Cancer Research Program to Dr. Qunwei Zhang. This work was also partly supported by P30ES030283 from the National Institute for Environmental Health Sciences (NIEHS).

Data availability statement

All data and materials are included in the manuscript.

Abbreviations

Nano-Co	Cobalt nanoparticles
HMGB1	High-mobility group box 1
DAMPs	Damage-associated molecular patterns
ECM	Extracellular matrix
TCA	Trichloroacetic acid
VHL	Von Hippel-Lindau
HIF-1α	Hypoxia inducible factor-1α

α-SMA	α-smooth muscle actin
RAGE	Receptor for advanced glycation end-products
MAPK	Mitogen-activated protein kinase
ERK	Extracellular regulating kinase
p38	p38 mitogen-activated protein kinase
JNK	c-Jun N-terminal kinase
CSE	Cigarette smoke extract

References

Adams TN, Butt YM, Batra K, and Glazer CS. 2017. "Cobalt related interstitial lung disease." Respir Med 129: 91–97. doi:10.1016/j.rmed.2017.06.008. [PubMed: 28732841]

Ahmedat AS, Warnken M, Seemann WK, Mohr K, Kostenis E, Juergens UR, and Racké K. 2013. "Pro-fibrotic processes in human lung fibroblasts are driven by an autocrine/paracrine endothelinergic system." Br J Pharmacol 168 (2): 471–87. doi:10.1111/j.1476-5381.2012.02190.x. [PubMed: 22935082]

Akbar M, Brewer JM, and Grant MH. 2011. "Effect of chromium and cobalt ions on primary human lymphocytes in vitro." J Immunotoxicol 8 (2): 140–9. doi:10.3109/1547691x.2011.553845. [PubMed: 21446789]

Al-Kuraishy HM, Al-Gareeb AI, Alkazmi L, Habotta OA, and Batiha GE. 2022. "High-mobility group box 1 (HMGB1) in COVID-19: extrapolation of dangerous liaisons." Inflammopharmacology 30 (3): 811–820. doi:10.1007/s10787-022-00988-y. [PubMed: 35471628]

Befani C, Mylonis I, Gkotinakou IM, Georgoulias P, Hu CJ, Simos G, and Liakos P. 2013. "Cobalt stimulates HIF-1-dependent but inhibits HIF-2-dependent gene expression in liver cancer cells." Int J Biochem Cell Biol 45 (11): 2359–68. doi:10.1016/j.biocel.2013.07.025. [PubMed: 23958427]

Brown C, Lacharme-Lora L, Mukonoweshuro B, Sood A, Newson RB, Fisher J, Case CP, and Ingham E. 2013. "Consequences of exposure to peri-articular injections of micro- and nano-particulate cobalt-chromium alloy." Biomaterials 34 (34): 8564–80. doi:10.1016/j.biomaterials.2013.07.073. [PubMed: 23932295]

Burgoyne RA, Fisher AJ, and Borthwick LA. 2021. "The Role of Epithelial Damage in the Pulmonary Immune Response." Cells 10 (10): doi:10.3390/cells10102763.

Cheng Y, Xiong J, Chen Q, Xia J, Zhang Y, Yang X, Tao K, Zhang S, and He S. 2017. "Hypoxia/reoxygenation-induced HMGB1 translocation and release promotes islet proinflammatory cytokine production and early islet graft failure through TLRs signaling." Biochim Biophys Acta Mol Basis Dis 1863 (2): 354–364. doi:10.1016/j.bbadis.2016.11.012. [PubMed: 27838489]

Dutz S, Buske N, Landers J, Gräfe C, Wende H, and Clement JH. 2020. "Biocompatible Magnetic Fluids of Co-Doped Iron Oxide Nanoparticles with Tunable Magnetic Properties." Nanomaterials (Basel) 10 (6): doi:10.3390/nano10061019.

Feng L, Zhang Y, Jiang M, Mo Y, Wan R, Jia Z, Tollerud DJ, Zhang X, and Zhang Q. 2015. "Up-regulation of Gadd45α after exposure to metal nanoparticles: the role of hypoxia inducible factor 1α." Environ Toxicol 30 (4): 490–9. doi:10.1002/tox.21926. [PubMed: 24277352]

Feng S, Zhang Z, Mo Y, Tong R, Zhong Z, Chen Z, He D, Wan R, Gao M, Mo Y, Zhang Q, and Huang Y. 2020. "Activation of NLRP3 inflammasome in hepatocytes after exposure to cobalt nanoparticles: The role of oxidative stress." Toxicol In Vitro 69: 104967. doi:10.1016/j.tiv.2020.104967. [PubMed: 32805375]

Gajjala PR, Kasam RK, Soundararajan D, Sinner D, Huang SK, Jegga AG, and Madala SK. 2021. "Dysregulated overexpression of Sox9 induces fibroblast activation in pulmonary fibrosis." JCI Insight 6 (20): doi:10.1172/jci.insight.152503.

Gao W, He R, Ren J, Zhang W, Wang K, Zhu L, and Liang T. 2021. "Exosomal HMGB1 derived from hypoxia-conditioned bone marrow mesenchymal stem cells increases angiogenesis via the JNK/HIF-1α pathway." FEBS Open Bio 11 (5): 1364–1373. doi:10.1002/2211-5463.13142.

Hamada N, Maeyama T, Kawaguchi T, Yoshimi M, Fukumoto J, Yamada M, Yamada S, Kuwano K, and Nakanishi Y. 2008. "The role of high mobility group box1 in pulmonary fibrosis." Am J Respir Cell Mol Biol 39 (4): 440–7. doi:10.1165/rcmb.2007-0330OC. [PubMed: 18441281]

He M, Kubo H, Ishizawa K, Hegab AE, Yamamoto Y, Yamamoto H, and Yamaya M. 2007. "The role of the receptor for advanced glycation end-products in lung fibrosis." Am J Physiol Lung Cell Mol Physiol 293 (6): L1427–36. doi:10.1152/ajplung.00075.2007. [PubMed: 17951314]

Hou C, Kong J, Liang Y, Huang H, Wen H, Zheng X, Wu L, and Chen Y. 2015. "HMGB1 contributes to allergen-induced airway remodeling in a murine model of chronic asthma by modulating airway inflammation and activating lung fibroblasts." Cell Mol Immunol 12 (4): 409–23. doi:10.1038/cmi.2014.60. [PubMed: 25152078]

IARC. 2023. "Volume 131: IARC Monographs on the Identification of Carcinogenic Hazards to Humans". In: Cobalt, Antimony Compounds, and Weapons-Grade Tungsten Alloy. International Agency for Research on Cancer © International Agency for Research on Cancer, 2023. For more information contact publications@iarc.fr., Lyon (FR).

Isshiki T, Naiel S, Vierhout M, Otsubo K, Ali P, Tsubouchi K, Yazdanshenas P, Kumaran V, Dvorkin-Gheva A, Kolb MRJ, and Ask K. 2024. "Therapeutic strategies to target connective tissue growth factor in fibrotic lung diseases." Pharmacol Ther 253: 108578. doi:10.1016/j.pharmthera.2023.108578. [PubMed: 38103794]

Jiang J, Wang GZ, Wang Y, Huang HZ, Li WT, and Qu XD. 2018. "Hypoxia-induced HMGB1 expression of HCC promotes tumor invasiveness and metastasis via regulating macrophage-derived IL-6." Exp Cell Res 367 (1): 81–88. doi:10.1016/j.yexcr.2018.03.025. [PubMed: 29571949]

Kadota T, Fujita Y, Araya J, Ochiya T, and Kuwano K. 2022. "Extracellular vesicle-mediated cellular crosstalk in lung repair, remodelling and regeneration." Eur Respir Rev 31 (163): doi:10.1183/16000617.0106-2021.

Kang R, Chen R, Zhang Q, Hou W, Wu S, Cao L, Huang J, Yu Y, Fan XG, Yan Z, Sun X, Wang H, Wang Q, Tsung A, Billiar TR, Zeh HJ 3rd, Lotze MT, and Tang D. 2014. "HMGB1 in health and disease." Mol Aspects Med 40: 1–116. doi:10.1016/j.mam.2014.05.001. [PubMed: 25010388]

Kawamura T, Singh Mallah G, Ardalan M, Chumak T, Svedin P, Jonsson L, Jabbari Shiadeh SM, Goretta F, Ikeda T, Hagberg H, Sandberg M, and Mallard C. 2023. "Therapeutic Effect of Nicotinamide Mononucleotide for Hypoxic-Ischemic Brain Injury in Neonatal Mice." ASN Neuro 15: 17590914231198983. doi:10.1177/17590914231198983. [PubMed: 37787108]

Kida T, Seno T, Nagahara H, Inoue T, Nakabayashi A, Kukida Y, Fujioka K, Fujii W, Wada M, Kohno M, and Kawahito Y. 2018. "Roles of high-mobility group box 1 and thrombin in murine pulmonary fibrosis and the therapeutic potential of thrombomodulin." Am J Physiol Lung Cell Mol Physiol 314 (3): L473–l483. doi:10.1152/ajplung.00287.2017. [PubMed: 29212801]

Kim JY, Lee EJ, Seo J, and Oh SH. 2017. "Impact of high-mobility group box 1 on melanocytic survival and its involvement in the pathogenesis of vitiligo." Br J Dermatol 176 (6): 1558–1568. doi:10.1111/bjd.15151. [PubMed: 27787879]

Kwon YM, Xia Z, Glyn-Jones S, Beard D, Gill HS, and Murray DW. 2009. "Dose-dependent cytotoxicity of clinically relevant cobalt nanoparticles and ions on macrophages in vitro." Biomed Mater 4 (2): 025018. doi:10.1088/1748-6041/4/2/025018. [PubMed: 19349653]

Lee K, Kang JE, Park SK, Jin Y, Chung KS, Kim HM, Lee K, Kang MR, Lee MK, Song KB, Yang EG, Lee JJ, and Won M. 2010. "LW6, a novel HIF-1 inhibitor, promotes proteasomal degradation of HIF-1alpha via upregulation of VHL in a colon cancer cell line." Biochem Pharmacol 80 (7): 982–9. doi:10.1016/j.bcp.2010.06.018. [PubMed: 20599784]

Lee K, Lee JH, Boovanahalli SK, Jin Y, Lee M, Jin X, Kim JH, Hong YS, and Lee JJ. 2007. "(Aryloxyacetylamino)benzoic acid analogues: A new class of hypoxia-inducible factor-1 inhibitors." J Med Chem 50 (7): 1675–84. doi:10.1021/jm0610292. [PubMed: 17328532]

Li W, Xu Q, Deng Y, Yang Z, Xing S, Zhao X, Zhu P, Wang X, He Z, and Gao Y. 2015. "High-mobility group box 1 accelerates lipopolysaccharide-induced lung fibroblast proliferation

in vitro: involvement of the NF-κB signaling pathway." Lab Invest 95 (6): 635–47. doi:10.1038/labinvest.2015.44. [PubMed: 25867768]

Lin X, Wang W, Chang X, Chen C, Guo Z, Yu G, Shao W, Wu S, Zhang Q, Zheng F, and Li H. 2024. "ROS/mtROS promotes TNTs formation via the PI3K/AKT/mTOR pathway to protect against mitochondrial damages in glial cells induced by engineered nanomaterials." Part Fibre Toxicol 21 (1): 1. doi:10.1186/s12989-024-00562-0. [PubMed: 38225661]

Lison D, De Boeck M, Verougstraete V, and Kirsch-Volders M. 2001. "Update on the genotoxicity and carcinogenicity of cobalt compounds." Occup Environ Med 58 (10): 619–25. doi:10.1136/oem.58.10.619. [PubMed: 11555681]

Middleton DRS, Wedekind R, Hall AL, Suonio E, DeBono N, Vermeulen R, Fritschi L, Stewart PA, and Schubauer-Berigan MK. 2024. "Critical reviews of exposure assessment in carcinogenic hazard identification: the IARC Monographs experience." Occup Environ Med: doi:10.1136/oemed-2023-109277.

Milikić J, Knežević S, Stojadinović S, Alsaiari M, Harraz FA, Santos DMF, and Šljukić B. 2022. "Facile Synthesis of Low-Cost Copper-Silver and Cobalt-Silver Alloy Nanoparticles on Reduced Graphene Oxide as Efficient Electrocatalysts for Oxygen Reduction Reaction in Alkaline Media." Nanomaterials (Basel) 12 (15): doi:10.3390/nano12152657.

Nemery B. 1990. "Metal toxicity and the respiratory tract." Eur Respir J 3 (2): 202–19. [PubMed: 2178966]

Osei ET, Noordhoek JA, Hackett TL, Spanjer AI, Postma DS, Timens W, Brandsma CA, and Heijink IH. 2016. "Interleukin-1α drives the dysfunctional cross-talk of the airway epithelium and lung fibroblasts in COPD." Eur Respir J 48 (2): 359–69. doi:10.1183/13993003.01911-2015. [PubMed: 27418555]

Peeters PM, Perkins TN, Wouters EF, Mossman BT, and Reynaert NL. 2013. "Silica induces NLRP3 inflammasome activation in human lung epithelial cells." Part Fibre Toxicol 10: 3. doi:10.1186/1743-8977-10-3. [PubMed: 23402370]

Peng T, Du SY, Son M, and Diamond B. 2021. "HIF-1α is a negative regulator of interferon regulatory factors: Implications for interferon production by hypoxic monocytes." Proc Natl Acad Sci U S A 118 (26): doi:10.1073/pnas.2106017118.

Perez JE, Van de Walle A, and Wilhelm C. 2020. "Versatile iron cobalt nanoparticles for theranostics." Nat Biomed Eng 4 (3): 252–253. doi:10.1038/s41551-020-0532-y. [PubMed: 32165733]

Perkins TN, and Oury TD. 2021. "The perplexing role of RAGE in pulmonary fibrosis: causality or casualty?" Ther Adv Respir Dis 15: 17534666211016071. doi:10.1177/17534666211016071. [PubMed: 34275342]

Polanská E, Dobšáková Z, Dvořáčková M, Fajkus J, and Štros M. 2012. "HMGB1 gene knockout in mouse embryonic fibroblasts results in reduced telomerase activity and telomere dysfunction." Chromosoma 121 (4): 419–31. doi:10.1007/s00412-012-0373-x. [PubMed: 22544226]

Rarick KR, Li K, Teng RJ, Jing X, Martin DP, Xu H, Jones DW, Hogg N, Hillery CA, Garcia G, Day BW, Naylor S, and Pritchard KA Jr. 2024. "Sterile inflammation induces vasculopathy and chronic lung injury in murine sickle cell disease." Free Radic Biol Med 215: 112–126. doi:10.1016/j.freeradbiomed.2024.01.052. [PubMed: 38336101]

Saint-Criq V, Villeret B, Bastaert F, Kheir S, Hatton A, Cazes A, Xing Z, Sermet-Gaudelus I, Garcia-Verdugo I, Edelman A, and Sallenave JM. 2018. "Pseudomonas aeruginosa LasB protease impairs innate immunity in mice and humans by targeting a lung epithelial cystic fibrosis transmembrane regulator-IL-6-antimicrobial-repair pathway." Thorax 73 (1): 49–61. doi:10.1136/thoraxjnl-2017-210298. [PubMed: 28790180]

Sakai N, and Tager AM. 2013. "Fibrosis of two: Epithelial cell-fibroblast interactions in pulmonary fibrosis." Biochim Biophys Acta 1832 (7): 911–21. doi:10.1016/j.bbadis.2013.03.001. [PubMed: 23499992]

Schmittgen TD, and Livak KJ. 2008. "Analyzing real-time PCR data by the comparative C(T) method." Nat Protoc 3 (6): 1101–8. doi:10.1038/nprot.2008.73. [PubMed: 18546601]

Shelfoon C, Shariff S, Traves SL, Kooi C, Leigh R, and Proud D. 2016. "Chemokine release from human rhinovirus-infected airway epithelial cells promotes fibroblast migration." J Allergy Clin Immunol 138 (1): 114–122.e4. doi:10.1016/j.jaci.2015.12.1308. [PubMed: 26883463]

Simm AO, Ji X, Banks CE, Hyde ME, and Compton RG. 2006. "AFM studies of metal deposition: instantaneous nucleation and the growth of cobalt nanoparticles on boron-doped diamond electrodes." Chemphyschem 7 (3): 704–9. doi:10.1002/cphc.200500557. [PubMed: 16514698]

Simonsen LO, Harbak H, and Bennekou P. 2012. "Cobalt metabolism and toxicology--a brief update." Sci Total Environ 432: 210–5. doi:10.1016/j.scitotenv.2012.06.009. [PubMed: 22732165]

Sims GP, Rowe DC, Rietdijk ST, Herbst R, and Coyle AJ. 2010. "HMGB1 and RAGE in inflammation and cancer." Annu Rev Immunol 28: 367–88. doi:10.1146/annurev.immunol.021908.132603. [PubMed: 20192808]

Sisler JD, Li R, McKinney W, Mercer RR, Ji Z, Xia T, Wang X, Shaffer J, Orandle M, Mihalchik AL, Battelli L, Chen BT, Wolfarth M, Andrew ME, Schwegler-Berry D, Porter DW, Castranova V, Nel A, and Qian Y. 2016. "Differential pulmonary effects of CoO and La2O3 metal oxide nanoparticle responses during aerosolized inhalation in mice." Part Fibre Toxicol 13 (1): 42. doi:10.1186/s12989-016-0155-3. [PubMed: 27527840]

Sohaebuddin SK, Thevenot PT, Baker D, Eaton JW, and Tang L. 2010. "Nanomaterial cytotoxicity is composition, size, and cell type dependent." Part Fibre Toxicol 7: 22. doi:10.1186/1743-8977-7-22. [PubMed: 20727197]

Su Z, Yin J, Wang T, Sun Y, Ni P, Ma R, Zhu H, Zheng D, Shen H, Xu W, and Xu H. 2014. "Up-regulated HMGB1 in EAM directly led to collagen deposition by a PKCβ/Erk1/2-dependent pathway: cardiac fibroblast/myofibroblast might be another source of HMGB1." J Cell Mol Med 18 (9): 1740–51. doi:10.1111/jcmm.12324. [PubMed: 24912759]

Thompson HG, Mih JD, Krasieva TB, Tromberg BJ, and George SC. 2006. "Epithelial-derived TGF-beta2 modulates basal and wound-healing subepithelial matrix homeostasis." Am J Physiol Lung Cell Mol Physiol 291 (6): L1277–85. doi:10.1152/ajplung.00057.2006. [PubMed: 16891397]

Thyssen JP 2012. "Cobalt sensitization and dermatitis: considerations for the clinician." Dermatitis 23 (5): 203–9. doi:10.1097/DER.0b013e31826e4591. [PubMed: 23010826]

Tohme S, Yazdani HO, Liu Y, Loughran P, van der Windt DJ, Huang H, Simmons RL, Shiva S, Tai S, and Tsung A. 2017. "Hypoxia mediates mitochondrial biogenesis in hepatocellular carcinoma to promote tumor growth through HMGB1 and TLR9 interaction." Hepatology 66 (1): 182–197. doi:10.1002/hep.29184. [PubMed: 28370295]

Wallace WA, and Howie SE. 1999. "Immunoreactive interleukin 4 and interferon-gamma expression by type II alveolar epithelial cells in interstitial lung disease." J Pathol 187 (4): 475–80. doi:10.1002/(sici)1096-9896(199903)187:4<475::Aid-path268>3.0.Co;2-n. [PubMed: 10398109]

Wan R, Mo Y, Feng L, Chien S, Tollerud DJ, and Zhang Q. 2012. "DNA damage caused by metal nanoparticles: involvement of oxidative stress and activation of ATM." Chem Res Toxicol 25 (7): 1402–11. doi:10.1021/tx200513t. [PubMed: 22559321]

Wan R, Mo Y, Zhang Z, Jiang M, Tang S, and Zhang Q. 2017. "Cobalt nanoparticles induce lung injury, DNA damage and mutations in mice." Part Fibre Toxicol 14 (1): 38. doi:10.1186/s12989-017-0219-z. [PubMed: 28923112]

Wang W, Zheng F, and Zhang A. 2021. "Arsenic-induced lung inflammation and fibrosis in a rat model: Contribution of the HMGB1/RAGE, PI3K/AKT, and TGF-β1/SMAD pathways." Toxicol Appl Pharmacol 432: 115757. doi:10.1016/j.taap.2021.115757. [PubMed: 34673086]

Wu Q, Feng Y, Ouyang Y, Liang Y, Zhao K, Wang Y, Luo Q, Xiao J, Feng N, and Zhou M. 2021. "Inhibition of advanced glycation endproducts formation by lotus seedpod oligomeric procyanidins through RAGE-MAPK signaling and NF-κB activation in high-AGEs-diet mice." Food Chem Toxicol 156: 112481. doi:10.1016/j.fct.2021.112481. [PubMed: 34375722]

Xu H, Ling M, Xue J, Dai X, Sun Q, Chen C, Liu Y, Zhou L, Liu J, Luo F, Bian Q, and Liu Q. 2018. "Exosomal microRNA-21 derived from bronchial epithelial cells is involved in aberrant epithelium-fibroblast cross-talk in COPD induced by cigarette smoking." Theranostics 8 (19): 5419–5433. doi:10.7150/thno.27876. [PubMed: 30555555]

Xue J, Patergnani S, Giorgi C, Suarez J, Goto K, Bononi A, Tanji M, Novelli F, Pastorino S, Xu R, Caroccia N, Dogan AU, Pass HI, Tognon M, Pinton P, Gaudino G, Mak TW, Carbone M, and Yang H. 2020. "Asbestos induces mesothelial cell transformation via HMGB1-driven autophagy." Proc Natl Acad Sci U S A 117 (41): 25543–25552. doi:10.1073/pnas.2007622117. [PubMed: 32999071]

Yang J, Pan X, Xu M, Li Y, Liang C, Liu L, Li Z, Wang L, and Yu G. 2024. "Downregulation of HMGCS2 mediated AECIIs lipid metabolic alteration promotes pulmonary fibrosis by activating fibroblasts." Respir Res 25 (1): 176. doi:10.1186/s12931-024-02816-z. [PubMed: 38658970]

Yap JMG, Ueda T, Kanemitsu Y, Takeda N, Fukumitsu K, Fukuda S, Uemura T, Tajiri T, Ohkubo H, Maeno K, Ito Y, Oguri T, Ugawa S, and Niimi A. 2021. "AITC inhibits fibroblast-myofibroblast transition via TRPA1-independent MAPK and NRF2/HO-1 pathways and reverses corticosteroids insensitivity in human lung fibroblasts." Respir Res 22 (1): 51. doi:10.1186/s12931-021-01636-9. [PubMed: 33579280]

Younus AR, Iqbal J, Muhammad N, Rehman F, Tariq M, Niaz A, Badshah S, Saleh TA, and Rahim A. 2019. "Nonenzymatic amperometric dopamine sensor based on a carbon ceramic electrode of type SiO(2)/C modified with Co(3)O(4) nanoparticles." Mikrochim Acta 186 (7): 471. doi:10.1007/s00604-019-3605-4. [PubMed: 31240490]

Yuan J, Mo Y, Zhang Y, Zhang Y, and Zhang Q. 2022. "Nickel nanoparticles induce epithelial-mesenchymal transition in human bronchial epithelial cells via the HIF-1α/HDAC3 pathway." Nanotoxicology 16 (6-8): 695–712. doi:10.1080/17435390.2022.2142169. [PubMed: 36345150]

Yuan J, Zhang Y, Zhang Y, Mo Y, and Zhang Q. 2021. "Effects of metal nanoparticles on tight junction-associated proteins via HIF-1α/miR-29b/MMPs pathway in human epidermal keratinocytes." Part Fibre Toxicol 18 (1): 13. doi:10.1186/s12989-021-00405-2. [PubMed: 33740985]

Zhang L, Ji Y, Kang Z, Lv C, and Jiang W. 2015. "Protocatechuic aldehyde ameliorates experimental pulmonary fibrosis by modulating HMGB1/RAGE pathway." Toxicol Appl Pharmacol 283 (1): 50–6. doi:10.1016/j.taap.2015.01.001. [PubMed: 25582705]

Zhang Q, Kusaka Y, and Donaldson K. 2000. "Comparative Pulmonary Responses Caused by Exposure to Standard Cobalt and Ultrafine Cobalt." Journal of Occupational Health 42 (4): 179–184. doi:10.1539/joh.42.179.

Zhang Y, Jiang M, Nouraie M, Roth MG, Tabib T, Winters S, Chen X, Sembrat J, Chu Y, Cardenes N, Tuder RM, Herzog EL, Ryu C, Rojas M, Lafyatis R, Gibson KF, McDyer JF, Kass DJ, and Alder JK. 2019. "GDF15 is an epithelial-derived biomarker of idiopathic pulmonary fibrosis." Am J Physiol Lung Cell Mol Physiol 317 (4): L510–l521. doi:10.1152/ajplung.00062.2019. [PubMed: 31432710]

Zhang Y, Mo Y, Zhang Y, Yuan J, and Zhang Q. 2023. "MMP-3-mediated cleavage of OPN is involved in copper oxide nanoparticle-induced activation of fibroblasts." Part Fibre Toxicol 20 (1): 22. doi:10.1186/s12989-023-00532-y. [PubMed: 37217992]

Zhang Y, Pan YD, Zheng WY, Li HY, Zhu MZ, Ou Yang WJ, Qian Y, Turecki G, Mechawar N, and Zhu XH. 2024. "Enhancing HIF-1α-P2X2 signaling in dorsal raphe serotonergic neurons promotes psychological resilience." Redox Biol 69: 103005. doi:10.1016/j.redox.2023.103005. [PubMed: 38150991]

Zhao J, Yu J, Xu Y, Chen L, Zhou F, Zhai Q, Wu J, Shu B, and Qi S. 2018. "Epidermal HMGB1 Activates Dermal Fibroblasts and Causes Hypertrophic Scar Formation in Reduced Hydration." J Invest Dermatol 138 (11): 2322–2332. doi:10.1016/j.jid.2018.04.036. [PubMed: 29787749]

Zou W, He F, Liu S, Pu J, Hu J, Sheng Q, Zhu T, Zhu T, Li B, and Ran P. 2018. "PM2.5 Induced the Expression of Fibrogenic Mediators via HMGB1-RAGE Signaling in Human Airway Epithelial Cells." Can Respir J 2018: 1817398. doi:10.1155/2018/1817398. [PubMed: 29670673]

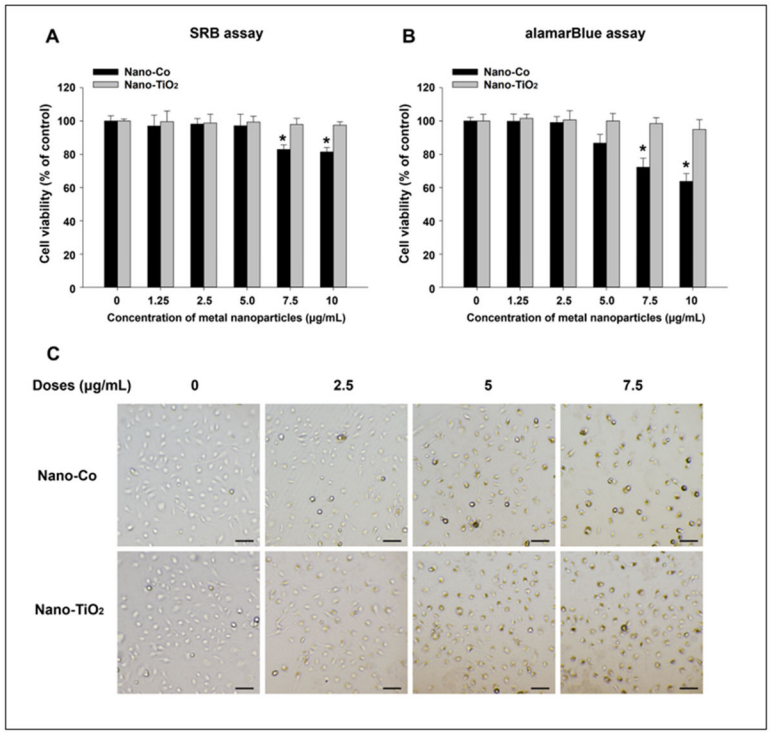

Figure 1. Cytotoxicity of metal nanoparticles on BEAS-2B cells.

$5x10^3$ cells per well were seeded in 96-well plates. After overnight culture, cells were treated with metal nanoparticles for 24 h. Cells without metal nanoparticle treatment were used as controls. Cytotoxicity was determined by SRB assay (A) or alamarBlue assay (B). Data are shown as mean ± SE ($n = 3$). *, $p < 0.01$ vs. Control. (C) Cell images were captured under a microscope (Olympus IX51). Scale bars represent 100 μm.

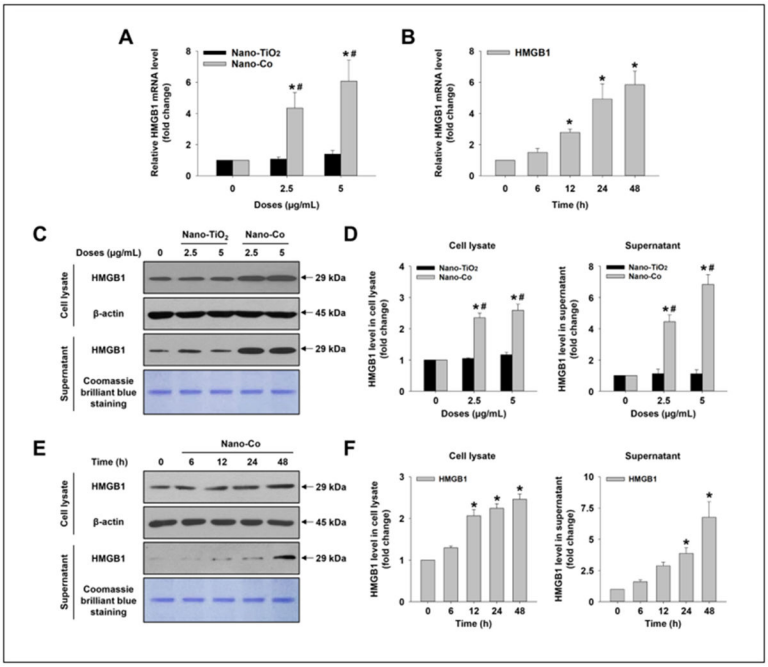

Figure 2. Dose- and time-dependent induction of HMGB1 expression and release in BEAS-2B cells exposed to Nano-Co.

BEAS-2B cells were exposed to 2.5 or 5 μg/mL of Nano-Co or Nano-TiO_2 for 24 h (A, C, D), or 5 μg/mL of Nano-Co for 6, 12, 24, and 48 h (B, E, F). Cells without treatment were used as control. (A-B) Expression of HMGB1 mRNA in BEAS-2B cells were determined by real-time PCR. (C-F) Western blot assay determined HMGB1 protein levels in cell lysate and supernatant. D and F are normalized band densitometry readings averaged from three independent experiments in C and E. β-actin and Coomassie Brilliant Blue stained gels served as loading controls. Data represent mean ± SE ($n = 3$). * Significant difference as compared with the control group, $p < 0.05$; # Significant difference as compared with the same dose of Nano-TiO_2-treated group, $p < 0.05$.

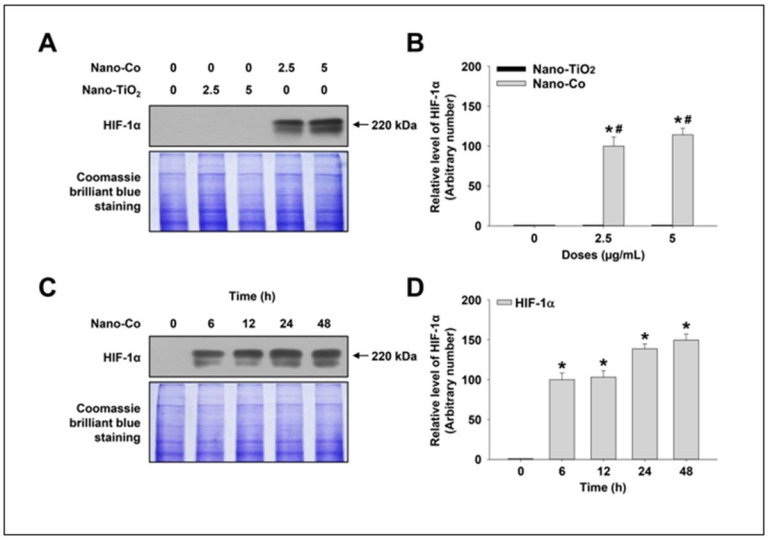

Figure 3. HIF-1α nuclear accumulation in BEAS-2B cells exposed to Nano-Co.

Expression of HIF-1α in BEAS-2B cells was determined by Western blot after cells were exposed to 2.5 or 5 μg/mL of Nano-Co or Nano-TiO_2 for 24 h (A, B), or to 5 μg/mL of Nano-Co for 6, 12, 24, or 48 h (C, D). Cells without treatment were used as control. B and D are normalized band densitometry readings averaged from three independent experiments of A and C. Coomassie Brilliant Blue stained gels served as loading controls. Data represent mean ± SE ($n = 3$). * Significant difference as compared with the control group, $p < 0.05$; # Significant difference as compared with the same dose of Nano-TiO_2-treated group, $p < 0.05$.

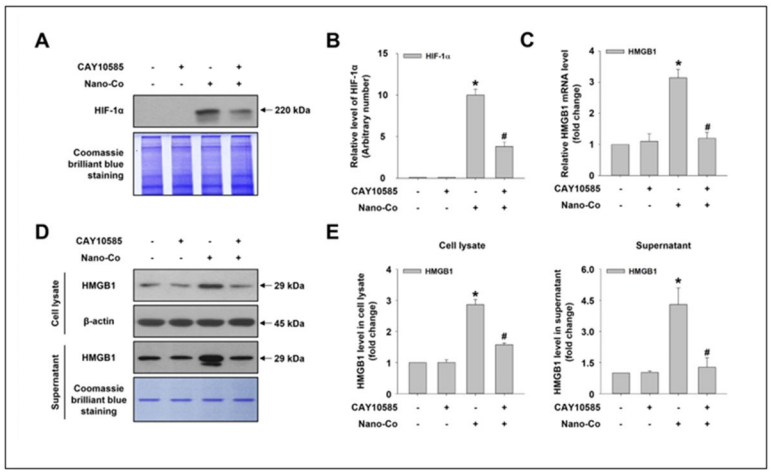

Figure 4. HIF-1α inhibition abolished Nano-Co-induced HMGB1 expression and release in BEAS-2B cells.

The cells were pretreated with 30 μM of CAY10585, a HIF-1α inhibitor, for 2 h prior to exposure to 5 μg/mL of Nano-Co for another 24 h. Cells without any treatments were used as control. (A-B) Expression of HIF-1α in cells was determined by Western blot. B is normalized band densitometry readings averaged from three independent experiments in A. (C) HMGB1 mRNA expression was determined by real-time PCR. (D-E) Expression of HMGB1 protein in cell lysate and supernatant was determined in Western blot. E is normalized band densitometry readings averaged from three independent experiments in D. β-actin and Coomassie Brilliant Blue stained gels served as loading controls. Data represent mean ± SE ($n = 3$). * Significant difference as compared with the control group, $p < 0.05$; # Significant difference as compared with the group with Nano-Co treatment, but without CAY10585 treatment, $p < 0.05$.

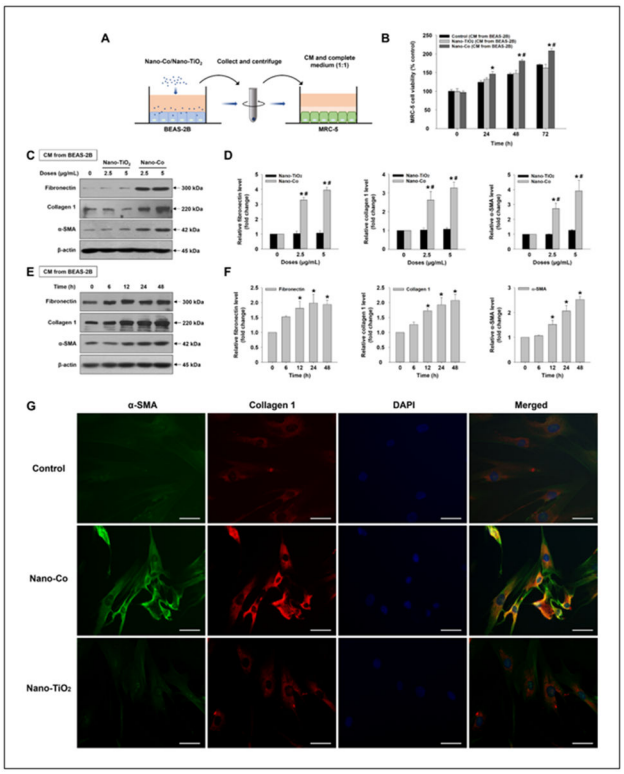

Figure 5. Conditioned medium from Nano-Co-exposed BEAS-2B cells induced the activation of MRC-5 cells.

A is the experiment protocol. (B) MTS assay measured the cell viability of MRC-5 cultured with the conditioned media from nanoparticle-exposed BEAS-2B (5 μg/mL x 24 h) for 24, 48, and 72 h. (C-F) Western blot assay determined the protein levels of fibrosis-associated proteins in MRC-5 cells cultured with conditioned media from BEAS-2B cells exposed to 2.5 or 5 μg/mL of Nano-TiO_2 or Nano-Co for 24 h (C-D), or exposed to 5 μg/mL of Nano-Co for 6, 12, 24, or 48 h (E-F). Cells without treatment were used as control. D and F are normalized band densitometry readings averaged from three independent experiments in C and E. β-actin served as loading controls. Data represent mean ± SE ($n = 3$). * Significant difference as compared with the control group, $p < 0.05$; # Significant difference as compared with the group with Nano-TiO_2 treatment, $p < 0.05$. (G) MRC-5 cells were cultured with the conditioned media from nanoparticle-exposed BEAS-2B (5 μg/mL x 24 h) for 48 h, and dual IF was performed. DAPI stains the nucleus of a cell. Scale bars represent 50 μm.

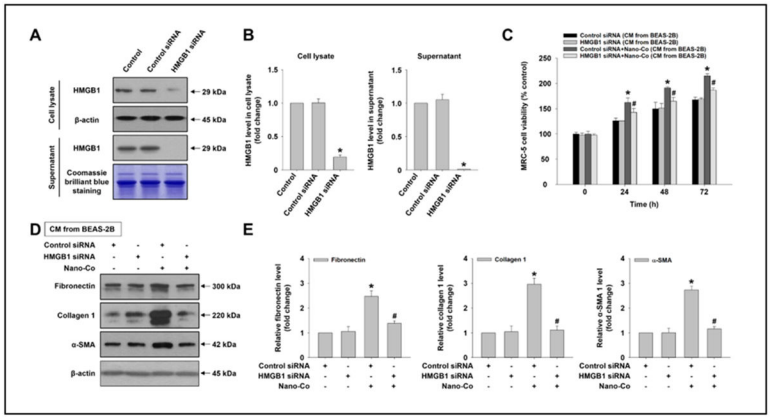

Figure 6. HMGB1-knockdown attenuated the activation of MRC-5 cells caused by conditioned medium from Nano-Co-exposed BEAS-2B cells.

(A-B) The effects of HMGB1 siRNA transfection on the production and release of HMGB1 in BEAS-2B cells were examined by Western blot. B is normalized band densitometry readings averaged from three independent experiments in A. (C) MTS assay measured the cell viability of MRC-5 cultured with conditioned medium from BEAS-2B cells transfected with or without HMGB1 siRNA for 24 h prior to 5 μg/mL of Nano-Co exposure for another 24 h. (D-E) Western blot assay measured the protein levels of fibrosis-associated proteins in MRC-5 cells cultured with conditioned media from BEAS-2B cells transfected with or without HMGB1 siRNA for 24 h prior to 5 μg/mL of Nano-Co exposure for another 24 h. E is normalized band densitometry readings averaged from three independent experiments in D. β-actin and Coomassie Brilliant Blue stained gels served as loading controls. Data represent mean ± SE ($n = 3$). * Significant difference as compared with the control or control siRNA group, $p < 0.05$; # Significant difference as compared with the control siRNA group with Nano-Co treatment, $p < 0.05$.

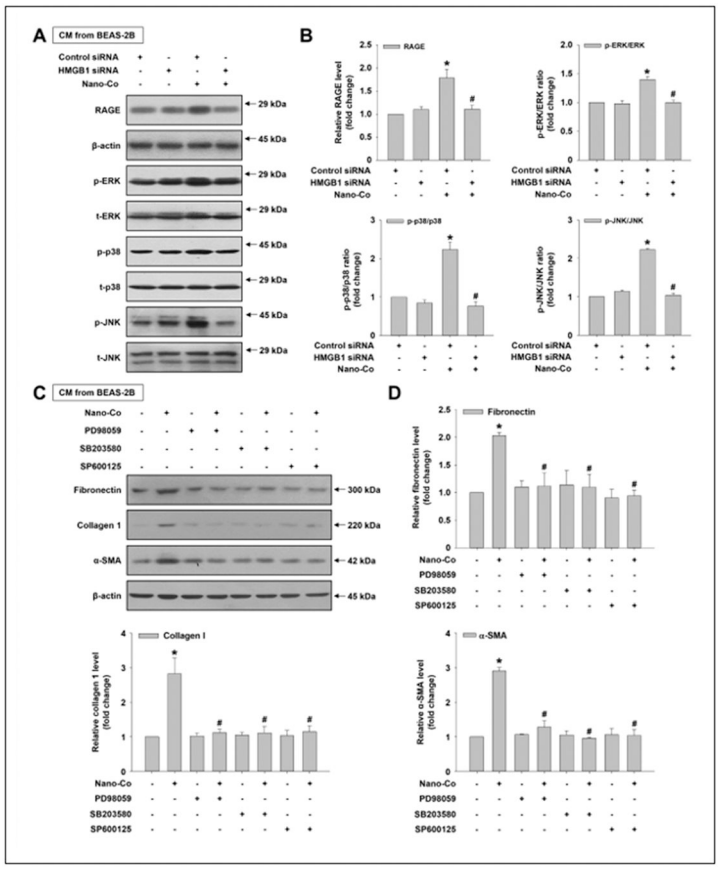

Figure 7. HMGB1 released from Nano-Co-exposed BEAS-2B cells activated MRC-5 cells via RAGE/MAPKs pathway.

(A-B) Western blot assay measured the protein levels of RAGE, phosphorylated and non-phosphorylated ERK, p38, and JNK in MRC-5 cells cultured with conditioned media from BEAS-2B cells transfected with or without HMGB1 siRNA for 24 h prior to 5 μg/mL of Nano-Co exposure for another 24 h. B is normalized band densitometry readings averaged from three independent experiments in A. (C-D) Western blot assay measured the protein levels of fibrosis-associated proteins in MRC-5 cells pre-incubated with 10 μM PD98059, SB203580, or SP600125 for 4 h prior to culture with conditioned media from BEAS-2B cells exposed to 5 μg/mL of Nano-Co for 24 h. D is normalized band densitometry readings averaged from three independent experiments in C. β-actin served as loading control. Data represent mean ± SE ($n = 3$). * Significant difference as compared with the control (without any treatments) or control siRNA only group, $p < 0.05$; # Significant difference as compared with Nano-Co only or Control siRNA+Nano-Co group, $p < 0.05$.

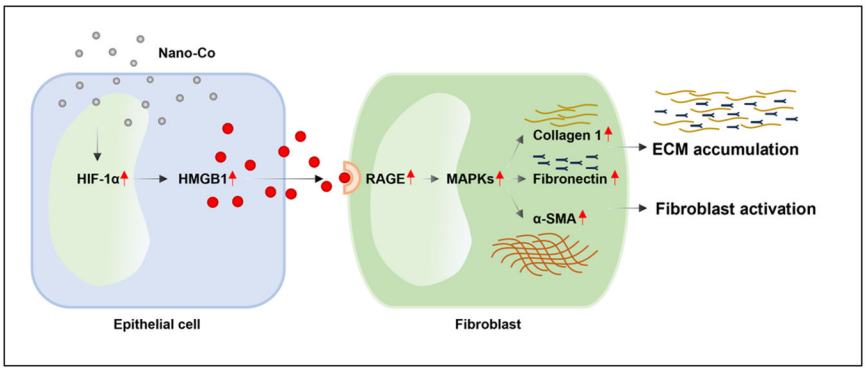

Figure 8. Schematic and potential mechanisms of Nano-Co-induced activation of lung fibroblasts.

Exposure of lung epithelial cells to Nano-Co causes increased expression and release of HMGB1 via a HIF-1α-dependent manner, which then promotes the activation of lung fibroblasts through RAGE-MAPKs pathway.